e-ISSN 2757-5195

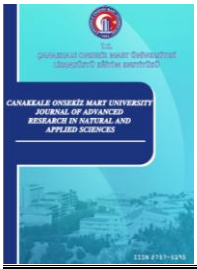

Çanakkale Onsekiz Mart University

Journal of Advanced Research in Natural and Applied Sciences

Open Access

doi.org/10.28979/jarnas.1111459 2022, Vol. 8, Issue 4, Pages: 762-776 dergipark.org.tr/tr/pub/jarnas

Fretting behavior of piston ring-cylinder liner components of a diesel engine running on TiO_2 nanolubricant

Ali Can Yılmaz[1,*]

[1]Department of Motor Vehicles and Transportation Technologies, Adana Vocational School, Cukurova University, Adana, Türkiye

Article History

Received: 30.04.2022

Accepted: 16.08.2022

Published: 15.12.2022

Research Article

Abstract − This experimental research presents the friction and wear characteristics of piston ring-cylinder liner component of a diesel engine running on commercial engine oil (5W-30) and TiO_2 nanoparticle (~20 nm, ≥99.5% trace metals basis) incorporated 5W-30 engine oil (nanolubricant) to observe the performance parameters in terms of mean effective pressures and smoke emissions. Dynamic light scattering was utilized to examine the nanoparticle dispersion in the lubricant. Thermo-gravimetric analysis on nanoparticles was conducted to examine the thermal endurance during abrasion tests. The samples directly cut from the spare piston ring of the test engine underwent severe friction and wear tests via linear friction module. Coefficient of friction was considered as comparison parameter to understand the tribological behavior of friction pairs submerged in two different lubricants. Scanning electron microscopy analysis was conducted to observe morphology of the nanoparticle and to analyze the surface structure of the samples before and after the abrasion tests. Atomic force microscopy analysis was done to obtain the 3D images of the worn surfaces and to make a comprehensive comparison of tribological performance between engine lubricant and nanolubricant. The results depicted that, TiO_2 is effective in reducing coefficient of friction by an average of 10.37% and wear rate by 33.58% as well as improving brake mean effective pressure by an average of 4.95% and reducing friction mean effective pressure by an average of 9.34% when compared to those of the engine oil. In parallel with reduced friction, TiO_2 incorporation in engine oil yielded an average reduction of 9.11% in smoke opacity. The experiments suggest promising results in terms of utilization of low friction, fuel efficient and environmental friendly internal combustion engines fulfilling strict emission regulations.

Keywords − *Diesel engine, mean effective pressure, smoke emission, tribology, TiO_2 nanoparticle;*

1. Introduction

Friction between solid surfaces in relative motion is a complex process due to wide variation in the magnitude of forces exerted onto the contact surfaces. Thus, various lubrication regimes occur in the piston ring-cylinder liner (PRCL) of a running engine. Basically, three regimes are observed in PRCL system: (i) Boundary lubrication generally occurs when the piston is at top dead center (TDC) and bottom dead center (BDC). The oil film is only formed by squeeze effect as the piston velocity is zero at these dead points. This causes thinner oil film at TDC and BDC, where fretting effects reach maximum. (ii) Hydrodynamic lubrication is expected to be seen at mid-strokes where higher piston velocity values are observed. As the piston moves, the lubrication ring distributes the lubricant on the cylinder liner. The oil film is thicker and metal-metal contact is minimum within mid-stroke region. (iii) Mixed lubrication represents the transition from boundary regime to hydrodynamic regime (Yin, Li, Fu, & Yun, 2012). Stribeck diagram is used to define lubrication regimes in which the Hersey number (HN) (1.1) is plotted against coefficient of friction. "f" can be expressed in terms of dry and hydrodynamic friction as depicted in 1.2 (Heywood, 2018):

[1] acyilmaz@cu.edu.tr

Corresponding Author

$$HN=\eta N/\Gamma \tag{1.1}$$
$$f=\sigma f_d+(1-\sigma)\ f_h \tag{1.2}$$

where;
η: dynamic viscosity of the lubricant (Pa.s)
N: entrainment speed of the lubricant (m/s)
Γ: loading force per length of the tribological contact (N/m)
σ: metal-metal contact constant ($0<\sigma<1$)
f_d: dry friction coefficient
f_h: hydrodynamic friction coefficient

As $\sigma\to1$ and $f\to f_d$, boundary friction occurs, that is, solid surfaces are nearly in contact (very thin oil layer in between). On the other hand, as $\sigma\to0$ and $f\to f_h$, hydrodynamic friction occurs where the thickness of the oil layer is adequate to fully separate the solid surfaces (Heywood, 2018).
In reciprocating engines, fretting pairs become deteriorated in time and piston ring assembly is responsible for 45% of total friction (Taylor, 1998). Thus, tribological characteristic of PRCL system is directly related to the lubrication performance of the engine (Dimkovski, Anderberg, Ohlsson, & Rosén, 2011; Guo, Yuan, Liu, Peng, & Yan, 2013).

Intriguing studies have been carried out by several researchers focusing on reducing frictional using various methods such as coating of contact surfaces (Kovalchenko, Ajayi, Erdemir, Fenske, & Etsion, 2005; Kumar, Sinha, & Agarwal, 2019; K. Y. Li, Zhou, Bello, Lee, & Lee, 2005; Lin, Wei, Bitsis, & Lee, 2016; Tung & Gao, 2003; Wróblewski & Koszalka, 2021), surface texturing (Kovalchenko et al., 2005; Podgornik, Vilhena, Sedlaček, Rek, & Žun, 2012; Ronen, Etsion, & Kligerman, 2001), organic friction modifiers as engine lubricant additives (Fry, Chui, Moody, & Wong, 2020; Guegan, Southby, & Spikes, 2019; Ratoi, Niste, Alghawel, Suen, & Nelson, 2014). Though undisputable advantageous features of these techniques in terms of reducing frictional losses within PRCL system, they may bring a huge cost burden to the researcher or his/her institution as they require expensive experimental set-ups. In this context, incorporation of nanoparticle additives in engine oil steps forward to improve the tribological behavior of PRCL pair, little amount of nanoparticle introduction into the engine oil is generally sufficient and very effective as well as requiring no special and high cost experimental set-ups. Furthermore, one does not need to make modifications on the test engine. Nanoparticles are characterized by their specific features that manipulate the lubrication mechanisms such as polishing (K. Lee et al., 2009), rolling (Liu et al., 2004), mending (Tao, Jiazheng, & Kang, 1996) and third body (Padgurskas, Rukuiza, Prosyčevas, & Kreivaitis, 2013) effects. Therefore, recently, metallic nanoparticles in elemental form such as Ag (Ghaednia, Babaei, Jackson, Bozack, & Khodadadi, 2013; J. Ma, Mo, & Bai, 2009), Cu (Hu, Peng, & Ding, 2013; Pan & Zhang, 2010; Wang, Yin, Zhang, Wang, & Zhao, 2013; Yang, Zhang, Zhang, Yu, & Zhang, 2013; Yu et al., 2008), Fe (Chen et al., 2015; S. Ma, Zheng, Cao, & Guo, 2010; Nabhan, Ghazaly, Mousa, & Rashed, 2020; Song et al., 2012; Yilmaz, 2020b, 2020a), Ni (Chou et al., 2010), Pd (Abad & Sánchez-López, 2013) or in compound form (Chen et al., 2015; Hernandez Battez et al., 2006; S. Ma et al., 2010; Nabhan et al., 2020; Song et al., 2012) have been studied by several researchers. Among nanoparticles as engine oil additives, TiO_2 nanoparticles have been attracting attention due to its higher corrosion endurance, wear resistance and thermal stability as well as entrainment ability onto the metal surface crevices (higher viscosity of nano-oil) to reduce friction (Cao et al., 2018; Ćurković, Ćurković, Salopek, Renjo, & Šegota, 2013; Dhiflaoui, Kaouther, & Larbi, 2018; Langlet et al., 2001; Wan, Chao, Liu, & Zhang, 2011).

Indicated mean effective pressure (IMEP) and brake mean effective pressure (BMEP) are useful parameters for comparison of engine performance. Researchers have been implementing valuable studies related to IMEP improvement such as developing fuel adjustment systems for CI engines (Shi, Sun, & Deng, 2016; Kokjohn, Hanson, Splitter, & Reitz, 2011; Bedoya, Saxena, Cadavid, Dibble, & Wissink, 2012), observation of fuel injection timing (Agarwal et al., 2013; Su, Ji, Wang, Shi, Yang, & Cong, 2017) and establishment of duel-fuel spark ignition engines running on various fuels (Liu, Wang, Long, & Wang, 2015). IMEP directly relates to the work done by engine and can be measured via optical pressure sensors (Nagashima, Kawa, & Tsuchiya,

2003) or it can be estimated as an area in a closed curve under P-V indication diagram using numerical integration. The average pressures in the engine cylinders are referred to as BMEP and it defines the work done by the crankshaft per swept volume as shown in 1.3 (Heywood, 2018; Pahmi et al., 2019):

$$BMEP=2*\pi*n*T/V_d \quad (1.3)$$

BMEP: brake mean effective pressure (Pa)
n: number of revolutions per power stroke (n=2 for 4-stroke engines)
T: brake torque (Nm)
V_d: displacement volume (m^3)

Friction mean effective pressure (FMEP) is another parameter defining the pressure loss between IMEP and BMEP due to friction occurring in the PRCL system. It is the mean effective pressure to overcome engine friction (Heywood, 2018). Thus, it is related to the lubrication conditions between contact surfaces and can be approximated by using 1.4:

$$FMEP=IMEP-BMEP \quad (1.4)$$

Smoke emissions (soot formation) are of great concern especially in diesel engines. Diesel engines are prone to emit smoke from the exhaust pipe under high loads due to lack of adequate oxygen to oxidize the most of the fuel (Abdullah, Abdullah, & Bhatia, 2008; Mishra & Prasad, 2014). Furthermore, at high loads, short ignition delay period (short time for mixing of air-fuel) at high fuel injection pressures deteriorate formation of homogeneous mixture, that is, increased smoke emissions (Celikten, 2003). Diesel particulate filter (DPF) has been a compulsory equipment in recent years to fulfill the strict emission regulations. DPFs are effective in reducing particulate matter (Nguyen, Sung, Lee, & Kim, 2011) and may be more effective with a reduction in frictional losses. Reducing frictional losses in PRCL system will make the engine deliver the same power with lesser fuel or more power with the same fuel amount yielding lower smoke emissions.

The goal of this study is to observe the tribological effects of TiO_2 nanolubricant on performance (IMEP, BMEP, FMEP) and smoke emissions of a diesel engine by conducting comprehensive friction and wear analyses on the samples made up of same material with the piston ring-cylinder liner components. Though there are several studies on tribological enhancement effects of TiO_2 nanoparticles as engine oil additive, literature review shows that no study has been conducted to investigate the performance and smoke emissions of a diesel engine running on TiO_2 nanolubricant. Furthermore, to the author's knowledge, no studies have been established related to the combination of tribological improvement of TiO_2 nanoparticles and in-cylinder mean effective pressure parameters as well as smoke emissions.

2. Experimental Procedure

In the first step of the study, scanning electron microscopy (SEM) analysis was carried out to observe the morphology of TiO_2 nanoparticles (~20 nm, ≥99.5% trace metals basis). In the next step, thermal stability (TG) analysis was carried out to investigate the thermal endurance of TiO_2 nanoparticles during friction tests under harsh conditions to determine any decomposition and/or deterioration at high temperatures. In the subsequent step, before friction tests, SEM image of sample surface (unworn cast iron sample directly cut from the spare piston ring of the test engine) was taken. Then, the sample was submerged in the engine oil and TiO_2 nano-oil ambients to undergo friction tests under the same experimental conditions (oil temperature, sliding distance, normal friction load exerted on the samples). Nanoparticle dispersion in engine oil has substantial effects on tribological performance as nanoparticle clusters formed in the oil are highly responsible for agglomeration between the contact surfaces. Therefore, it is essential to prepare a nano-oil in which the nanoparticles suspend homogeneously. Firstly, the nanoparticle incorporated lubricant was ultrasonicated for 1 h to make a homogeneous dispersion of the nanoparticles. Dynamic light scattering (DLS) technique was utilized to confirm the homogenous dispersion of the nanoparticles in the oil. DLS is one of the most widely used techniques for detecting size distributions, dispersion, and morphologies of dry and powdered nanoparticles in liquids. It uses a He–Ne laser operating at a certain wavelength (651 nm for this study) and a detection angle (174^{o} for this study) (Murdock, Braydich-Stolle, Schrand, Schlager, & Hussain, 2008; Pecora, 2000). The beam coming out of the laser source is focused on the nano-oil suspension via a lens and scattered beams from the nanoparticles are detected by a high speed camera. A software computes the zeta potential (ζ-p) value from the beam data detected by the camera and processed by a data acquisition system (Figure 1). Zeta potential defines the particle agglomeration, sedimentation, contact and complexation of nanoparticles with other media elements in suspension and this value must be higher than 30 mV for a stable and homogeneous nano-oil (Krishna Sabareesh, Gobinath, Sajith, Das, & Sobhan, 2012; J. H. Lee et al., 2008; Strenge, 1995). Average ζ–p value of nanolubricant was over 30 mV even 10 days after its preparation. Technical specifications of the DLS device is tabulated in Table 1. Experiments showed that TiO_2 incorporation in engine oil above 0.5 wt.% causes sedimentation on the sample surface and coefficient of friction (CoF) tends to depict a sharp increase. Thus, 0.5 wt.% was considered as the nanoparticle amount in the engine oil during experiments. Subsequent to friction tests, worn sample surfaces were SEM analysed to compare the surface images before and after the fretting trials. Atomic force microscopy (AFM) analyses were also implemented on sample surfaces before and after the abrasion tests to observe wear characteristics. At the beginning of the friction tests, samples were cleaned in diluted HCl bath to get rid of contaminations. Then, the surfaces were washed with pure water and blown by nitrogen gas (drying process). The normal force during abrasion tests was maintained at 40 N due to excessive damage formed on the sample surface. The specifications of the friction test conditions are given in Table 2.

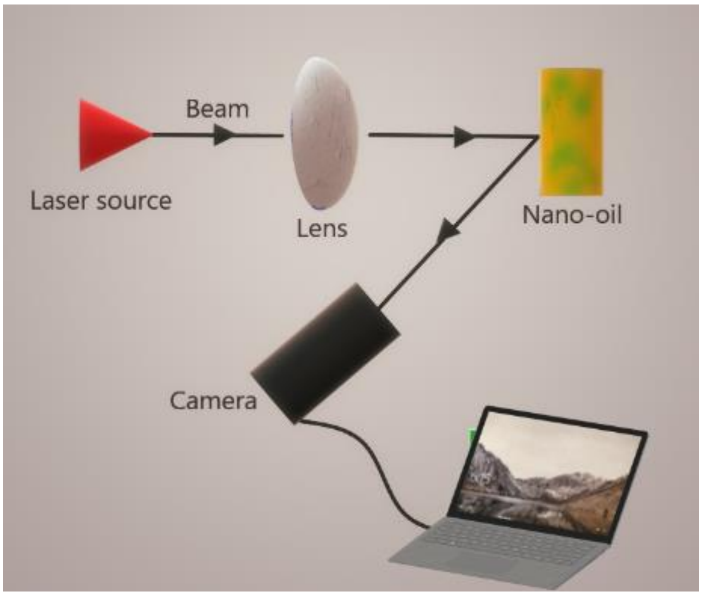

Figure 1. Illustration of DLS technique

Table 1
DLS device technical specifications

Diameter measurement range	3.8–100 μm
Mobility range	±20 μcm/Vs
Zeta potential range	>±500 mV
Measurement sensitivity	±2 mV
Beam	He-Ne laser
Motion capture	CCD camera
Minimum sample volume	12 μL
Maximum conductivity	200 mS/cm
Zeta potential measurement	15 days after its preparation

Table 2
Friction test specifications

Sample material	Cast iron
Sample size (LxWxH)	20x20x4 mm
Module motion	Reciprocating
Scratcher	Steel ball (Ø5 mm)
Scratcher linear speed	2000 mm/min
Scratcher distance travelled	200 m
TiO_2 mass fraction	0.5 wt.%
Oil bath temperature	25ºC
Normal load	40 N
Oil vessel volume	150 mL

The final stage of the study includes the single cylinder 4-stroke diesel engine tests with normal 5W-30 engine oil and TiO_2 incorporated (0.5 wt.%) engine oil (nano-oil). The comparison of these two lubricants in terms of in-cylinder mean effective pressures and smoke emissions was also conducted. The technical specifications of the test engine are shown in Table 3.

Table 3
Technical data of the single cylinder water cooled diesel test engine

Air induction	Naturally aspirated
Fuel feeding system	Direct injection
Bore	85 mm
Stroke	78 mm
Displacement	481 cc
Compression ratio	18:1
Lubrication	Pump in oil sump
Max. rev.	3200 rpm
Max. power	7.8 kW@2800 rpm
Max. torque	29.5 Nm@1850 rpm
Mass	55 kg

During running of the engine, each instantaneous pressure value was measured via a piezoelectric pressure sensor (Table 4) and transferred to the software by a data acquisition system. The crank angle corresponding to instantaneous volume values was also measured utilizing a crank sensor which is connected to the same data acquisition system. Thus, each instantaneous pressure datum subtending to each instantaneous crank angle was recorded. Then, crank angle values were approximately converted to the corresponding volume data. The area under the closed loop P-V diagram gives the net indicated work which is computed via cyclic integration of the piston work (P.dV). In other words, IMEP can be defined as the net indicated work per swept volume (V_s) as presented in 2.1:

$$IMEP=[1/V_s][\oint P.dV] \tag{2.1}$$

Table 4
Technical data of the piezoelectric pressure sensor

Measuring range	0-300 bar
Sensitivity	-30 pC/bar
Natural frequency	≥65 kHz
Operating temp. range	-20–1560ºC
Capacitance (no cables)	12 pF
Connector	10-32 UNF

The test engine was loaded via electromagnetic forces utilizing an eddy current dynamometer with arm length of 185 mm. Each engine test was carried out at normal engine operating temperature, same ambient temperature (25ºC) and relative humidity (55%) under wide open pumping (max. rpm at 0% load) conditions. The loading process was done gradually until the engine starts to stammer. A digital smokemeter with ±1% precision was used to measure the smoke opacity. The device was initially calibrated with checks at 0% and 100% smoke opacity. General schematic of the test rig is demonstrated in Figure 2.

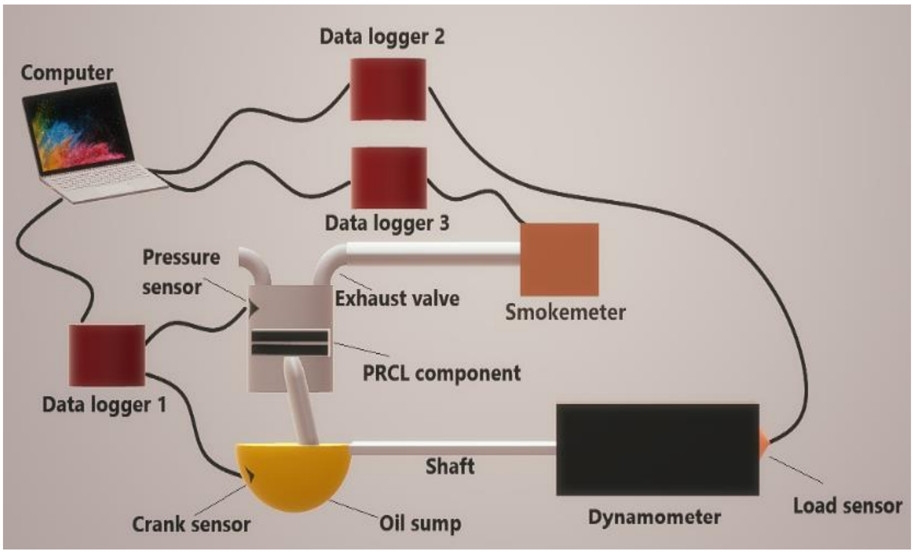

Figure 2. Schematic of the test rig

3. Results and Discussion

3.1. Morphology and thermo-gravimetric (TG) analysis

Nanoparticle geometry highly affects the friction and wear characteristics between contact surfaces (Zhang, Hu, Feng, & Wang, 2013). In general, the geometry is spherical throughout the structure (Figure 3) and rolling effect is expected to be dominant in reducing friction between solid pairs at moderate lubricant temperatures.

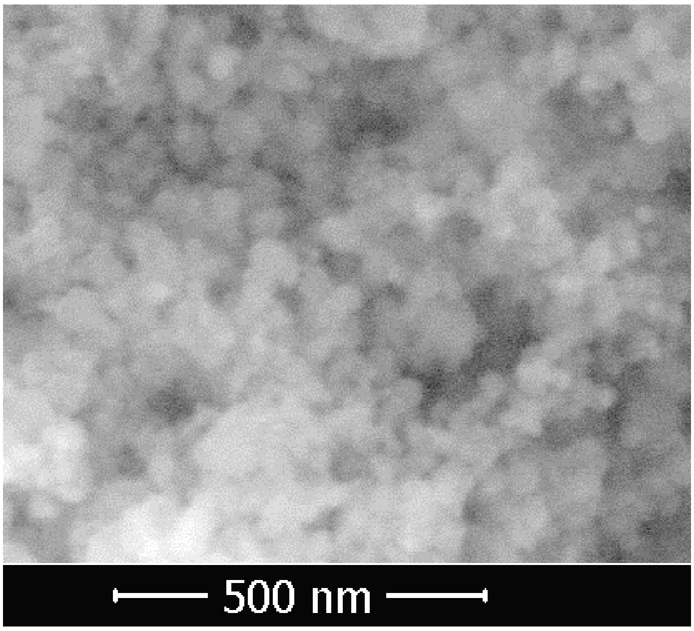

Figure 3. SEM image of TiO_2 nanoparticles

Thermo-gravimetric methods reveal the changes in the structure of nanoparticles as a result of temperature variations. Chemical reactions, polymerization, and crystallization processes are commonly represented by exothermic peaks, while phase shifts, dehydration, degradation, and reduction reactions are represented by endothermic peaks. The lack of peaks suggests that the sample's thermal stability is high, implying that no degradation during the work performed at that temperature range (Ali et al., 2016; Peng, Hu, & Wang, 2007; Zin et al., 2014). As can be seen in Figure 4, TiO_2 nanoparticles were able to perform high resistance to harsh thermal conditions even above 600ºC (no sharp peaks). Mass increase with the increase in temperature is related to the oxidation of metals on the surface during the heating process in an oxygen-rich environment. Mass loss with increased temperature, on the other hand, may signal a possible breakdown response (S. Li & Bhushan, 2016).

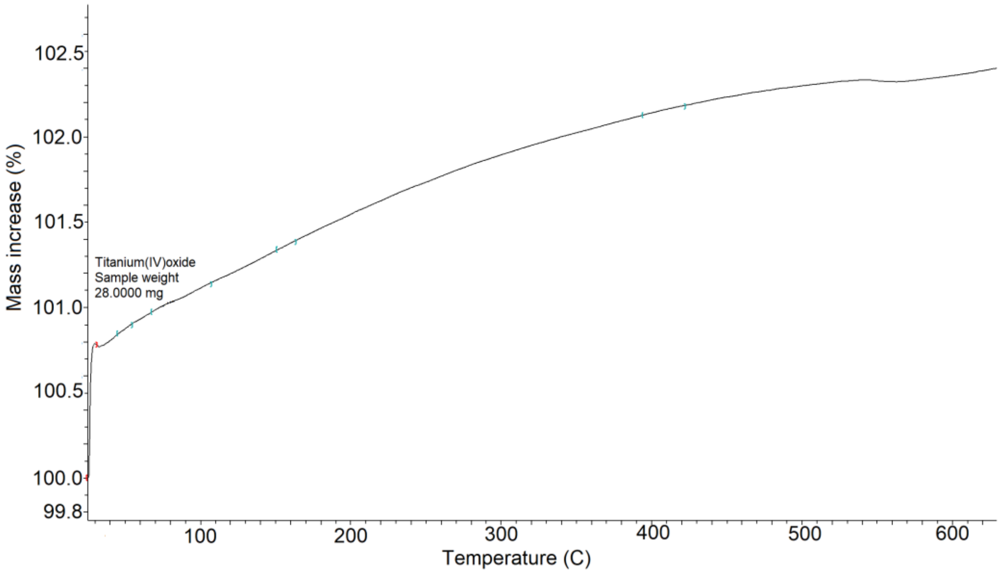

Figure 4. Thermo-gravimetric behavior of the TiO_2 nanoparticles

3.2. Friction and wear analysis

Friction between two solid surfaces can be reduced by either lowering the contact surface area (rolling effect) or decreasing the surface roughness (polishing effect). The CoF data procured from the linear friction module are depicted in Figure 5. For both lubricant modes, mixed lubrication (transition from boundary to hydrodynamic) can be observed until approximately sliding distance of 200 m. As of 200 m, hydrodynamic friction occurs due to increase in shear stress in oil film arising from high scratcher velocity at mid-strokes (mid-sliding distance). The average CoF in TiO_2 nano-oil is 10.37% lower than that of neat 5W-30 engine oil. The reduction in CoF is due to: (i) the spherical shape of TiO_2 nanoparticles which reveals the rolling effect and extra separation influence on fretting pairs, (ii) average zeta potential of 85 mV of the nano-oil that confirms the homogeneous dispersion of nanoparticles in the engine oil, ensuring smoother operation, (iii) filling of asperities with nano size TiO_2 particles yielding polishing effect and smoother contact regions, (iv) higher viscosity of nano-oil that provides more stable tribofilm between friction pairs and increase in load bearing capacity.

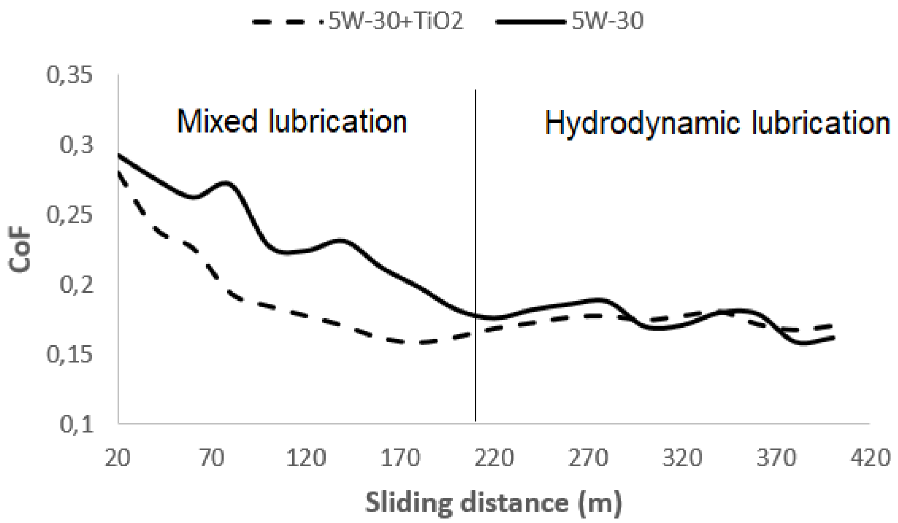

Figure 5. CoF with respect to sliding distance

Wear analysis on friction pairs is based on SEM (Figure 6) and AFM (Figure 7) images of surfaces before and after abrasion tests. The wear rate and surface roughness data (Table 5) were also collected to make a comprehensive wear study. It is clearly seen from both SEM and AFM results that the surface of the specimen submerged in the nano-oil is smoother than the one in the engine oil. The average surface roughness (R_a) experiments were conducted in triplicate and average of these values were taken into account. The SEM image of the unworn surface was shown to make a before-after comparison. For nano-oil ambient, average reductions of 33.58% and 15.85% were determined in wear rate and average R_a, respectively. Higher viscosity of nano-oil yields a slight increase in pressure of oil film and thus, separation of contact surfaces. Lower average CoF values for nano-oil also confirm this phenomenon. Reduced wear tracks on the surface submerged in nano-oil ambient may also be explained based on TG results (no melting at even high temperatures). High thermal endurance of TiO_2 nanoparticles provides maintenance of spherical geometry and rolling effect. Furthermore, polishing effect of nano size particles favors reduced wear tracks.

Table 5
Wear and average surface roughness test results

Lubricant	**Wear rate (mm^3/Nm)**	**R_a (µm)**			**Average R_a (µm)**
		Test 1	Test 2	Test 3	
5W-30	32.28×10^{-9}	0.92	0.81	0.73	0.82
5W-30+TiO_2	21.44×10^{-9}	0.84	0.72	0.51	0.69
Reduction	**33.58%**				**15.85%**

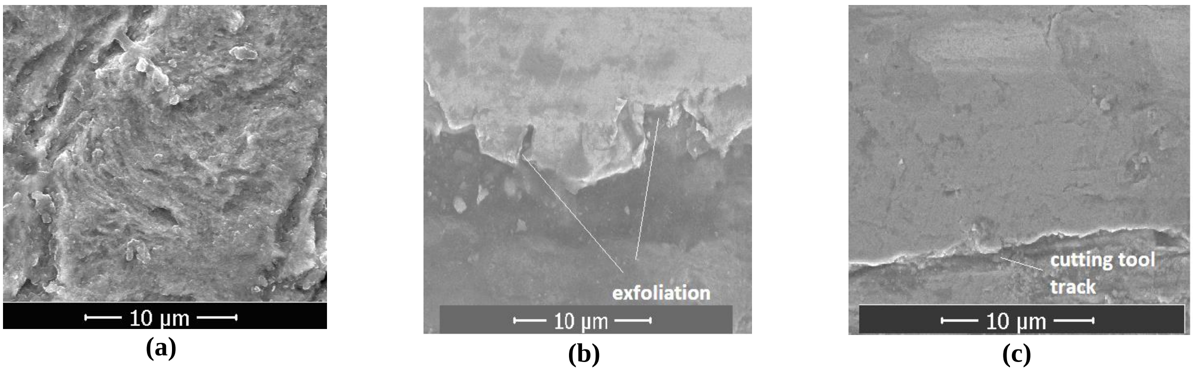

Figure 6. SEM images of (a) unworn raw sample surface, (b) worn sample surface in engine oil, (c) worn sample surface in TiO_2 nano-oil

3D-AFM images of the unworn and worn surfaces also clearly confirm that wear rate (mass loss) is higher in engine oil than that of nano-oil according to the average surface roughness height shown in vertical axis. Smoother surface is clearly observed on the sample underwent friction tests in nano-oil than that of engine oil. The “plains” are dominant compared to ”hills” on the surface processed in nano-oil. The small amount of sharp points on the images are due to AFM gain oscillation measurement errors.

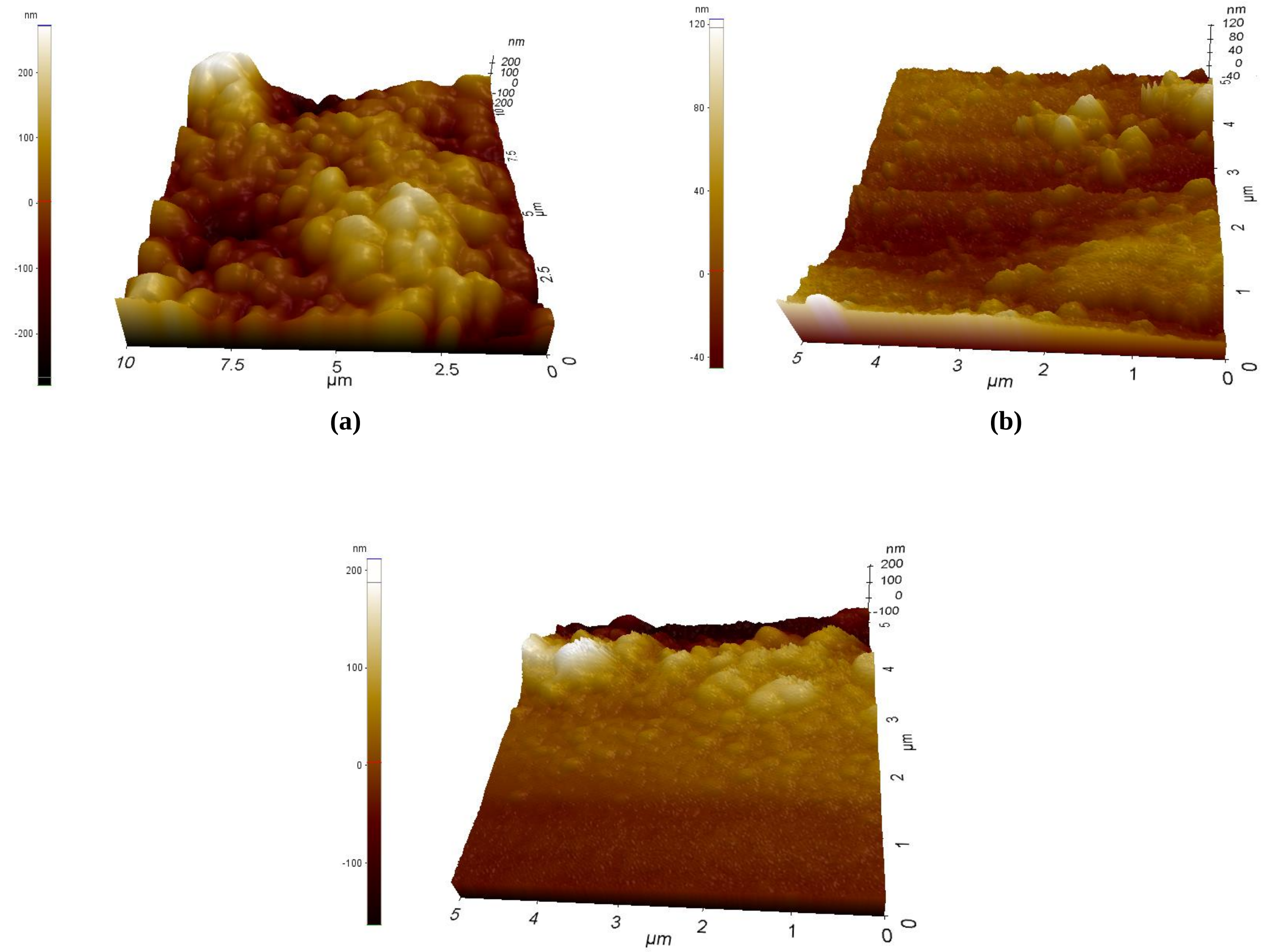

(a) (b) (c)

Figure 7. 3D-AFM images of (a) unworn raw sample surface, (b) worn sample surface in engine oil, (c) worn sample surface in TiO_2 nano-oil

3.3. Mean effective pressure and smoke emission analyses

In-cylinder IMEP is a good comparison parameter in terms of combustion efficiency and work done by combustion force exerted onto the piston head. This study includes the indirect determination of IMEP using P-V indicator diagram (Figure 8) plotted by means of the data taken from the pressure and crank sensors. Each volume datum subtending to each crank angle was recorded as mentioned in the previous section. The area integration of the closed loop gives the net indicated work delivered by the engine and IMEP is calculated using 2.1 as depicted above.

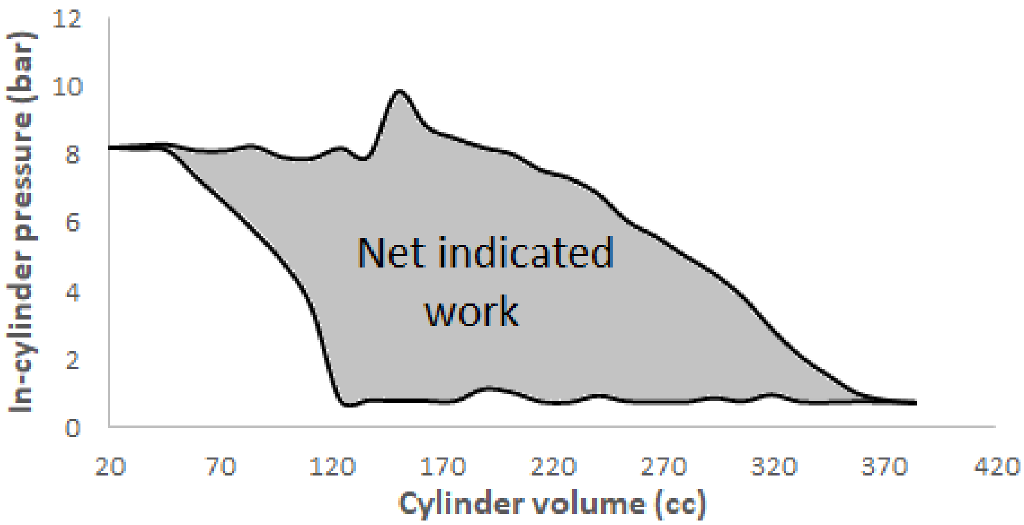

Figure 8. P-V indicator diagram of the engine

BMEP was used as another performance comparison parameter for the test engine running on two lubricant modes. Dynamometer load cell provides the torque values corresponding to each engine speed via data logger and a software. BMEP data were obtained substituting in 1.3. To observe the effects of fretting behavior on mean pressure drops due to frictions, FMEP data were also computed considering the difference between IMEP and BMEP (1.4). Mean effective pressure values were plotted against engine speed as seen in Figure 9. Torque is prone to increase until mid-revs and reaches maximum at about 2000 rpm due to development of mixture (more time for fuel to participate combustion). As approaching mid-revs, developed mixture unites with lower heat loss, thus maximum torque is achieved. Above 2000 rpm, torque tends to decrease as there was very insufficient time for combustion due to short opening time of intake valve. Recalling the direct proportion between torque and BMEP, the same trend is expected for BMEP. FMEP stands for the mean pressure loss and, hence, is inversely proportional to BMEP. Minimum FMEP is expected where the BMEP reaches its maximum and vice versa. Especially at high revs, an escalation in FMEP increase rate was observed which can be ascribed to elevated shear stress in tribofilm between fretting pairs.

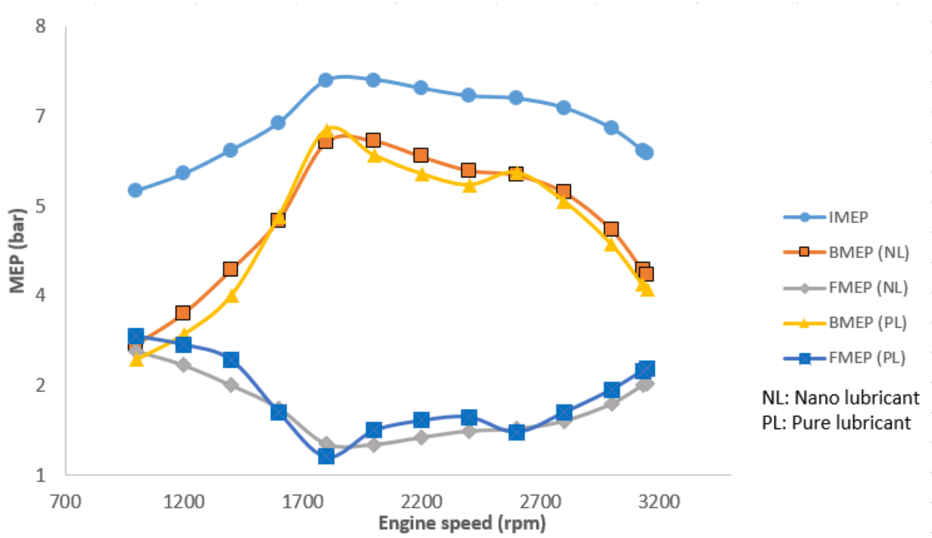

Figure 9. Mean effective pressures vs. engine speed for both lubrication modes

Smoke emission is one of the biggest problem of diesel engines due to its environmental and health hazards. Figure 10 demonstrates the variation of smoke opacity with respect to engine speed. As the load increases (rpm decreases), more fuel is to be injected into the combustion chamber to overcome the inverse forces exerted by the dynamometer. If there is no adequate time for sufficient air to enter the cylinder, some of the fuel will not find air for oxidation and combustion will remain incomplete causing unburned solid fuel particles in the exhaust system. Reducing fretting forces entails smooth engine operation in which the injectors will spray lesser fuel to overcome the decreased frictional forces and thus, lower smoke emissions. Improved tribological features of the TiO_2 nanolubricant is the main reason in reducing smoke in comparison to that of the neat engine oil.

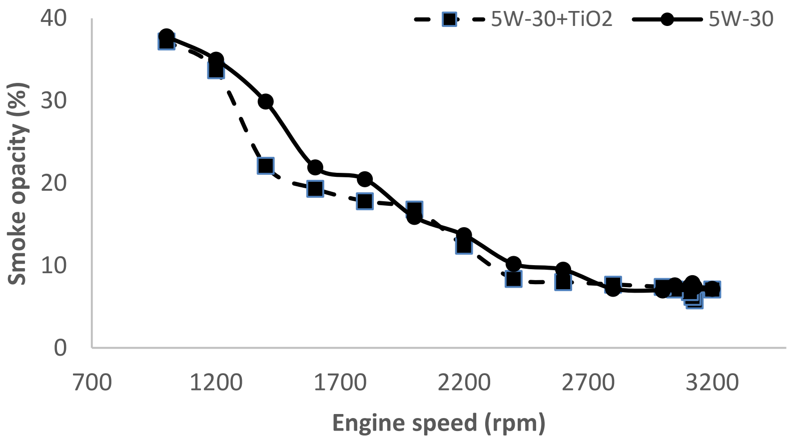

Figure 10. Variation of smoke opacity with respect to engine speed

4. Conclusions

This experimental study reveals the tribological improvement features of TiO_2 nanoparticle incorporation in commercial engine oil in the context of reducing frictional losses between PRCL components of a single cylinder diesel engine via comprehensive analyses. The results prove the effectiveness of TiO_2 nanoparticles in engine oil in terms of reducing frictional losses, enhancing performance and decreasing smoke emissions. The results seem to be promising due to attainment of 10.37% reduction in CoF, 4.95% improvement in BMEP, 9.34% and 9.11% reductions in FMEP and smoke emissions, respectively. Furthermore, TiO_2 nanolubricant provides reductions of 15.85% and 33.58% in surface roughness and wear rate, respectively. High thermal resistance of TiO_2 nanoparticles also facilitates its usage in engine oil, as very severe conditions may exist in the PRCL system of an internal combustion engine especially at the end of compression and at the time of combustion in which pressure and temperature reach very high levels.

Acknowledgment

This study was conducted in Cukurova University, Adana Vocational School, Automotive Laboratories and fiscally supported by Cukurova University, Scientific Research Projects, under Grant number FBA-2021-14009.

Author Contributions

Ali Can Yılmaz: Participation in the concept, design, analysis, writing, and revision of the manuscript.

Conflict of interest

The author declares no conflict of interest.

References

Abad, M. D., & Sánchez-López, J. C. (2013). Tribological properties of surface-modified Pd nanoparticles for electrical contacts. *Wear, 297*(1–2), 943–951. doi: https://doi.org/10.1016/j.wear.2012.11.009

Abdullah, A. Z., Abdullah, H., & Bhatia, S. (2008). Improvement of loose contact diesel soot oxidation by synergic effects between metal oxides in K_2O-V_2O_5/ZSM-5 catalysts. *Catalysis Communications, 9*(6), 1196–1200. doi: https://doi.org/10.1016/j.catcom.2007.11.003

Agarwal, A. K., Srivastava, D. K., Dhar, A., Maurya, R. K., Shukla, P.C., & Singh, A. P. (2013). Effect of fuel injection timing and pressure on combustion, emissions and performance characteristics of a single cylinder diesel engine. *Fuel*, *111*, 374-383, doi: 10.1016/j.fuel.2013.03.016

Ali, M. K. A., Xianjun, H., Mai, L., Bicheng, C., Turkson, R. F., & Qingping, C. (2016). Reducing frictional power losses and improving the scuffing resistance in automotive engines using hybrid nanomaterials as nano-lubricant additives. *Wear, 364–365*, 270–281. doi: https://doi.org/10.1016/j.wear.2016.08.005

Bedoya, I. D., Saxena, S., Cadavid, F. J., Dibble, R. W., & Wissink, M. (2011). Experimental study of biogas combustion in an HCCI engine for power generation with high indicated efficiency and ultra-low NO_x emissions. *Energy Conversion and Management, 53*(1), 154-162. doi: 10.1016/j.enconman.2011.08.016

Cao, L., Liu, J., Wan, Y., Yang, S., Gao, J., & Pu, J. (2018). Low-friction carbon-based tribofilm from poly-alpha-olefin oil on thermally oxidized Ti_6Al_4V. *Surface and Coatings Technology, 337*, 471–477. doi: https://doi.org/10.1016/j.surfcoat.2018.01.057

Çelikten, I. (2003). An experimental investigation of the effect of the injection pressure on engine performance and exhaust emission in indirect injection diesel engines. *Applied Thermal Engineering, 23*(16), 2051–2060. doi: https://doi.org/10.1016/S1359-4311(03)00171-6

Chen, B., Gu, K., Fang, J., Jiang, W., Jiu, W., & Nan, Z. (2015). Tribological characteristics of monodispersed cerium borate nanospheres in biodegradable rapeseed oil lubricant. *Applied Surface Science, 353*, 326–332. doi: https://doi.org/10.1016/j.apsusc.2015.06.107

Chou, R., Battez, A. H., Cabello, J. J., Viesca, J. L., Osorio, A., & Sagastume, A. (2010). Tribological behavior of polyalphaolefin with the addition of nickel nanoparticles. *Tribology International, 43*(12), 2327–2332. doi: https://doi.org/10.1016/j.triboint.2010.08.006

Ćurković, L., Ćurković, H. O., Salopek, S., Renjo, M. M., & Šegota, S. (2013). Enhancement of corrosion protection of AISI 304 stainless steel by nanostructured sol-gel TiO_2 films. *Corrosion Science, 77*, 176–184. doi: https://doi.org/10.1016/j.corsci.2013.07.045

Dhiflaoui, H., Kaouther, K., & Larbi, A. B. C. (2018). Wear behavior and mechanical properties of TiO_2 coating deposited electrophoretically on 316 L stainless steel. *Journal of Tribology, 140*(3). DOI: https://doi.org/10.1115/1.4038102

Dimkovski, Z., Anderberg, C., Ohlsson, R., & Rosén, B. G. (2011). Characterization of worn cylinder liner surfaces by segmentation of honing and wear scratches. *Wear, 271*(3–4), 548–552. doi: https://doi.org/10.1016/j.wear.2010.04.024

Fry, B. M., Chui, M. Y., Moody, G., & Wong, J. S. S. (2020). Interactions between organic friction modifier additives. *Tribology International, 151*. DOI: https://doi.org/10.1016/j.triboint.2020.106438

Ghaednia, H., Babaei, H., Jackson, R. L., Bozack, M. J., & Khodadadi, J. M. (2013). The effect of nanoparticles on thin film elasto-hydrodynamic lubrication. *Applied Physics Letters, 103*(26). doi: https://doi.org/10.1063/1.4858485

Guegan, J., Southby, M., & Spikes, H. (2019). Friction Modifier Additives, Synergies and Antagonisms. *Tribology Letters, 67*(3). doi: https://doi.org/10.1007/s11249-019-1198-z

Guo, Z., Yuan, C., Liu, P., Peng, Z., & Yan, X. (2013). Study on influence of cylinder liner surface texture on lubrication performance for cylinder liner-piston ring components. *Tribology Letters, 51*(1), 9–23. doi: https://doi.org/10.1007/s11249-013-0141-y

Hernandez Battez, A., Fernandez Rico, J. E., Navas Arias, A., Viesca Rodriguez, J. L., Chou Rodriguez, R., & Diaz Fernandez, J. M. (2006). The tribological behaviour of ZnO nanoparticles as an additive to PAO6. *Wear, 261*(3–4), 256–263. doi: https://doi.org/10.1016/j.wear.2005.10.001

Heywood, J. B. (2018). Internal Combustion Engine Fundamentals, Second Edition. In Internal Combustion Engine Fundamentals Second Edition. Retrieved from https://www.accessengineeringlibrary.com/content/book/9781260116106%0

Hu, H., Peng, H., & Ding, G. (2013). Nucleate pool boiling heat transfer characteristics of refrigerant/ nanolubricant mixture with surfactant. *International Journal of Refrigeration, 36*(3), 1045–1055. doi: https://doi.org/10.1016/j.ijrefrig.2012.12.015

Kokjohn, S. L., Hanson, R. M., Splitter, D. A., & Reitz, R. D. (2011). Fuel reactivity controlled compression ignition (RCCI): a pathway to controlled high-efficiency clean combustion. *International Journal of Engine Research, 12*(3), 209-226. doi: 10.1177/1468087411401548

Kovalchenko, A., Ajayi, O., Erdemir, A., Fenske, G., & Etsion, I. (2005). The effect of laser surface texturing on transitions in lubrication regimes during unidirectional sliding contact. *Tribology International, 38*(3), 219–225. doi: https://doi.org/10.1016/j.triboint.2004.08.004

Krishna Sabareesh, R., Gobinath, N., Sajith, V., Das, S., & Sobhan, C. B. (2012). Application of TiO_2 nanoparticles as a lubricant-additive for vapor compression refrigeration systems - An experimental investigation. *International Journal of Refrigeration, 35*(7), 1989–1996. doi: https://doi.org/10.1016/j.ijrefrig.2012.07.002

Kumar, V., Sinha, S. K., & Agarwal, A. K. (2019). Wear evaluation of engine piston rings coated with dual layer hard and soft coatings. *Journal of Tribology, 141*(3). doi: https://doi.org/10.1115/1.4041762

Langlet, M., Burgos, M., Coutier, C., Jimenez, C., Morant, C., & Manso, M. (2001). Low temperature preparation of high refractive index and mechanically resistant sol-gel TiO_2 films for multilayer antireflective coating applications. *Journal of Sol-Gel Science and Technology, 22*(1–2), 139–150. doi: https://doi.org/10.1023/A:1011232807842

Lee, J. H., Hwang, K. S., Jang, S. P., Lee, B. H., Kim, J. H., Choi, S. U. S., & Choi, C. J. (2008). Effective viscosities and thermal conductivities of aqueous nanofluids containing low volume concentrations of Al_2O_3 nanoparticles. *International Journal of Heat and Mass Transfer, 51*(11–12), 2651–2656. doi: https://doi.org/10.1016/j.ijheatmasstransfer.2007.10.026

Lee, K., Hwang, Y., Cheong, S., Choi, Y., Kwon, L., Lee, J., & Kim, S. H. (2009). Understanding the role of nanoparticles in nano-oil lubrication. *Tribology Letters, 35*(2), 127–131. doi: https://doi.org/10.1007/s11249-009-9441-7

Li, K. Y., Zhou, Z. F., Bello, I., Lee, C. S., & Lee, S. T. (2005). Study of tribological performance of ECR-CVD diamond-like carbon coatings on steel substrates Part 1. The effect of processing parameters and operating conditions. *Wear, 258*(10), 1577–1588. doi: https://doi.org/10.1016/j.wear.2004.10.006

Li, S., & Bhushan, B. (2016). Lubrication performance and mechanisms of Mg/Al-, Zn/Al-, and Zn/Mg/Al-layered double hydroxide nanoparticles as lubricant additives. *Applied Surface Science, 378*, 308–319. doi: https://doi.org/10.1016/j.apsusc.2016.03.220

Lin, J., Wei, R., Bitsis, D. C., & Lee, P. M. (2016). Development and evaluation of low friction TiSiCN nanocomposite coatings for piston ring applications. *Surface and Coatings Technology, 298*, 121–131. doi: https://doi.org/10.1016/j.surfcoat.2016.04.061

Liu, G., Li, X., Qin, B., Xing, D., Guo, Y., & Fan, R. (2004). Investigation of the mending effect and mechanism of copper nano-particles on a tribologically stressed surface. *Tribology Letters, 17*(4), 961–966. doi: https://doi.org/10.1007/s11249-004-8109-6

Liu, H., Wang, Z., Long, Y., & Wang, J. (2015). Dual-Fuel Spark Ignition (DFSI) combustion fuelled with different alcohols and gasoline for fuel efficiency. *Fuel, 157*, 255-260. doi: 10.1016/j.fuel.2015.04.042

Ma, J., Mo, Y., & Bai, M. (2009). Effect of Ag nanoparticles additive on the tribological behavior of multialkylated cyclopentanes (MACs). *Wear, 266*(7–8), 627–631. doi: https://doi.org/10.1016/j.wear.2008.08.006

Ma, S., Zheng, S., Cao, D., & Guo, H. (2010). Anti-wear and friction performance of ZrO_2 nanoparticles as lubricant additive. *Particuology, 8*(5), 468–472. doi: https://doi.org/10.1016/j.partic.2009.06.007

Mishra, A., & Prasad, R. (2014). Preparation and application of perovskite catalysts for diesel soot emissions control: An overview. *Catalysis Reviews - Science and Engineering, 56*, 57–81. doi: https://doi.org/10.1080/01614940.2014.866438

Murdock, R. C., Braydich-Stolle, L., Schrand, A. M., Schlager, J. J., & Hussain, S. M. (2008). Characterization of nanomaterial dispersion in solution prior to in vitro exposure using dynamic light scattering technique. *Toxicological Sciences, 101*(2), 239–253. doi: https://doi.org/10.1093/toxsci/kfm240

Nabhan, A., Ghazaly, N. M., Mousa, H. M., & Rashed, A. (2020). Influence of TiO_2 and SiO_2 nanoparticles additives on the engine oil tribological properties: Experimental study at different operating conditions. *International Journal of Advanced Science and Technology, 29*(1), 845–855.

Nagashima, K., Kawa, T., & Tsuchiya, K. (2003). Indicated mean effective pressure measuring method using optical fiber pressure sensor. *SAE Technical Papers*. doi: https://doi.org/10.4271/2003-01-2013

Nguyen, L. D. K., Sung, N. W., Lee, S. S., & Kim, H. S. (2011). Effects of split injection, oxygen enriched air and heavy EGR on soot emissions in a diesel engine. *International Journal of Automotive Technology, 12*(3), 339–350. DOI: https://doi.org/10.1007/s12239-011-0040-x

Padgurskas, J., Rukuiza, R., Prosyčevas, I., & Kreivaitis, R. (2013). Tribological properties of lubricant additives of Fe, Cu and Co nanoparticles. *Tribology International, 60*, 224–232. doi: https://doi.org/10.1016/j.triboint.2012.10.024

Pahmi, A., Hisyam Basri, M., Mustaffa, M. E., Yaakob, Y., Sharudin, H., Ismail, N. I., & Talib, R. J. (2019). Intake pressure and brake mean effective pressure analysis on various intake manifold design. *Journal of Physics: Conference Series, 1349*(1). doi: https://doi.org/10.1088/1742-6596/1349/1/012080

Pan, Q., & Zhang, X. (2010). Synthesis and tribological behavior of oil-soluble cu nanoparticles as additive in SF15W/40 lubricating oil. *Xiyou Jinshu Cailiao Yu Gongcheng/Rare Metal Materials and Engineering, 39*(10), 1711–1714. doi: https://doi.org/10.1016/s1875-5372(10)60129-4

Pecora, R. (2000). Dynamic light scattering measurement of nanometer particles in liquids. *Journal of Nanoparticle Research, 2*(2), 123–131. DOI: https://doi.org/10.1023/A:1010067107182

Peng, Y., Hu, Y., & Wang, H. (2007). Tribological behaviors of surfactant-functionalized carbon nanotubes as lubricant additive in water. *Tribology Letters, 25*(3), 247–253. doi: https://doi.org/10.1007/s11249-006-9176-7

Podgornik, B., Vilhena, L. M., Sedlaček, M., Rek, Z., & Žun, I. (2012). Effectiveness and design of surface texturing for different lubrication regimes. *Meccanica, 47*(7), 1613–1622. doi: https://doi.org/10.1007/s11012-012-9540-7

Ratoi, M., Niste, V. B., Alghawel, H., Suen, Y. F., & Nelson, K. (2014). The impact of organic friction modifiers on engine oil tribofilms. *RSC Advances, 4*(9), 4278–4285. doi: https://doi.org/10.1039/c3ra46403b

Ronen, A., Etsion, I., & Kligerman, Y. (2001). Friction-reducing surface-texturing in reciprocating automotive components. *Tribology Transactions, 44*(3), 359–366. doi: https://doi.org/10.1080/10402000108982468

Shi, L., Sun, Y., & Deng, K. (2016). Fuel adjustment to achieve a smooth net indicated mean effective pressure during mode switching from homogeneous charge compression ignition to conventional diesel compression ignition in a transient hydrocarbon emissions study. *Proceedings of the Institution of Mechanical Engineers, Part D: Journal of Automobile Engineering, 230*(13), 1758-1766. doi: 10.1177/0954407015623408

Song, X., Zheng, S., Zhang, J., Li, W., Chen, Q., & Cao, B. (2012). Synthesis of monodispersed $ZnAl_2O_4$ nanoparticles and their tribology properties as lubricant additives. *Materials Research Bulletin, 47*(12), 4305–4310. doi: https://doi.org/10.1016/j.materresbull.2012.09.013

Strenge, K. (1995). Introduction to Modern Colloid Science. *Zeitschrift Für Physikalische Chemie, 189*(2), 277–278. doi: https://doi.org/10.1524/zpch.1995.189.part_2.277a

Su, T., Ji, C., Wang, S., Shi, L., Yang, J., & Cong, X. (2017). Effect of spark timing on performance of a hydrogen-gasoline rotary engine. *Energy Conversion and Management, 148*, 120-127. doi: 10.1016/j.enconman.2017.05.064

Tao, X., Jiazheng, Z., & Kang, X. (1996). The ball-bearing effect of diamond nanoparticles as an oil additive. *Journal of Physics D: Applied Physics, 29*(11), 2932–2937. doi: https://doi.org/10.1088/0022-3727/29/11/029

Taylor, C. M. (1998). Automobile engine tribology-design considerations for efficiency and durability. *Wear, 221*(1), 1–8. doi: https://doi.org/10.1016/S0043-1648(98)00253-1

Tung, S. C., & Gao, H. (2003). Tribological characteristics and surface interaction between piston ring coatings and a blend of energy-conserving oils and ethanol fuels. *Wear, 255*(7–12), 1276–1285. doi: https://doi.org/10.1016/S0043-1648(03)00240-0

Wan, Y., Chao, W., Liu, Y., & Zhang, J. (2011). Tribological performance of Fluoroalkylsilane modification of sol-gel TiO_2 coating. *Journal of Sol-Gel Science and Technology, 57*(2), 193–197. doi: https://doi.org/10.1007/s10971-010-2341-3

Wang, X. L., Yin, Y. L., Zhang, G. N., Wang, W. Y., & Zhao, K. K. (2013). Study on antiwear and repairing performances about mass of nano-copper lubricating additives to 45 steel. *Physics Procedia, 50*, 466–472. doi: https://doi.org/10.1016/j.phpro.2013.11.073

Wróblewski, P., & Koszalka, G. (2021). An Experimental Study on Frictional Losses of Coated Piston Rings with Symmetric and Asymmetric Geometry. *SAE International Journal of Engines, 14*(6). doi: https://doi.org/10.4271/03-14-06-0051

Yang, G., Zhang, Z., Zhang, S., Yu, L., & Zhang, P. (2013). Synthesis and characterization of highly stable dispersions of copper nanoparticles by a novel one-pot method. *Materials Research Bulletin, 48*(4), 1716–1719. doi: https://doi.org/10.1016/j.materresbull.2013.01.025

Yilmaz, A. C. (2020a). Performance evaluation of a refrigeration system using nanolubricant. *Applied Nanoscience (Switzerland), 10*(5), 1667–1678. doi: https://doi.org/10.1007/s13204-020-01258-5

Yilmaz, A. C. (2020b). Tribological Enhancement Features of Various Nanoparticles as Engine Lubricant Additives: An Experimental Study. *Arabian Journal for Science and Engineering, 45*(2), 1125–1134. doi: https://doi.org/10.1007/s13369-019-04243-5

Yin, B., Li, X., Fu, Y., & Yun, W. (2012). Effect of laser textured dimples on the lubrication performance of cylinder liner in diesel engine. *Lubrication Science, 24*(7), 293–312. doi: https://doi.org/10.1002/ls.1185

Yu, H., Xu, Y., Shi, P., Xu, B., Wang, X., & Liu, Q. (2008). Tribological properties and lubricating mechanisms of Cu nanoparticles in lubricant. *Transactions of Nonferrous Metals Society of China (English Edition), 18*(3), 636–641. doi: https://doi.org/10.1016/S1003-6326(08)60111-9

Zhang, S., Hu, L., Feng, D., & Wang, H. (2013). Anti-wear and friction-reduction mechanism of Sn and Fe nanoparticles as additives of multialkylated cyclopentanes under vacuum condition. *Vacuum, 87*, 75–80. doi: https://doi.org/10.1016/j.vacuum.2012.07.009

Zin, V., Agresti, F., Barison, S., Colla, L., Mercadelli, E., Fabrizio, M., & Pagura, C. (2014). Tribological properties of engine oil with carbon nano-horns as nano-additives. *Tribology Letters, 55*(1), 45–53. doi: https://doi.org/10.1007/s11249-014-0330-3